Journal of Functional Foods 109 (2023) 105813

Contents lists available at ScienceDirect

Journal of Functional Foods

journal homepage: www.elsevier.com/locate/jff

Ultrasound-assisted pumpkin tendril extracts inhibits melanogenesis by suppressing the CREB/MITF signaling pathway in B16F10 melanoma cells, zebrafish, and a human skin model

Sujung Hong [a], Sojeong Lee [a], Woo-Jin Sim [a], Wook Chul Kim [b], Seon-Young Kim [c], Mi Hee Park [c], Wonchul Lim [d,*], Tae-Gyu Lim [a,d,*]

[a] Department of Food Science & Biotechnology, Sejong University, Seoul 05006, Republic of Korea
[b] Department of Medical Science, Soonchunhyang University, Asan 31538, Republic of Korea
[c] Jeonju AgroBio-Materials Institute, Jeonju-si, 54810, Republic of Korea
[d] Department of Food Science & Biotechnology, and Carbohydrate Bioproduct Research Center, Sejong University, Seoul 05006, Republic of Korea

ARTICLE INFO

Keywords:
Melanin Production
Pumpkin Tendril Extract
Reconstituted Human Tissues
Skin-whitening
Zebrafish

ABSTRACT

Agricultural byproducts are intermediate products generated during food processing and contain functional ingredients that are suitable for use in the green circular economy. This study aimed to demonstrate the skin-whitening effect of pumpkin tendril extract (PTE) using a mushroom tyrosinase assay, L-DOPA staining, qRT-PCR, western blotting, a zebrafish model, and a reconstituted 3D human skin model. PTE dose-dependently scavenged DPPH free radicals and inhibited melanogenesis stimulated by α-MSH without exhibiting cytotoxicity in 2D- and 3D-cultured B16F10 cells. Interestingly, PTE significantly reduced melanogenesis in zebrafish and 3D-pigmented human skin models. In addition, PTE notably downregulated the expression of proteins related to melanogenesis, such as MITF, TRP-1, TRP-2, and tyrosinase. Phosphorylation of CREB, an upregulator of MITF, was also attenuated by PTE treatment. Component analysis revealed that rutin is an active compound in PTE affecting melanogenesis. These results suggest that PTE suppresses melanogenesis and tyrosinase activity by regulating the CREB/MITF signaling pathway.

1. Introduction

Melanin is a pigment synthesized in melanocytes located in the basal layer of the skin that determines skin color (Yamaguchi, Brenner, & Hearing, 2007). An adequate amount of melanin can protect against the harmful effects of external environmental factors such as ultraviolet (UV) radiation (Solano, 2020). However, excessive melanin production owing to UV exposure can cause pigmentation, staining, and skin cancer. The signaling pathway related to melanogenesis is initiated by several factors, including cyclic adenosine monophosphate (cAMP), protein kinase A (PKA), and cAMP response element-binding protein (CREB). Tyrosinase synthesizes melanin by sequentially converting tyrosine into L-3,4-dihydroxyphenylalanine (L-DOPA) and L-DOPA quinone. During melanogenesis, microphthalmia-associated transcription factor (MITF) regulates melanin formation by controlling tyrosinase, tyrosinase-related protein 1 (TRP-1), and tyrosinase-related protein 2 (TRP-2) (D'Mello, Finlay, Baguley, & Askarian-Amiri, 2016). Accordingly, evaluation of melanogenesis-related enzyme activity and transcription factor expression levels is widely used as an indicator to identify ingredients for skin whitening.

Ultrasound-assisted extraction (UAE) is an alternative method for extracting bioactive compounds in a short time at low temperatures with low energy and solvent requirements. UAE is a non-thermal extraction technique suitable for retaining the functionality of bioactive

Abbreviations: UV, ultraviolet; cAMP, cyclic adenosine monophosphate; PKA, protein kinase A; CREB, cAMP response element-binding protein; L-DOPA, L-3,4-dihydroxyphenylalanine; MITF, microphthalmia-associated transcription factor; TRP, tyrosinase-related protein; UAE, ultrasound-assisted extraction; DPPH, 2,2-diphenyl-1-picrylhydrazyl, α-MSH, α-melanocyte stimulating hormone; PTE, pumpkin tendril extract.

* Corresponding authors at: Department of Food Science & Biotechnology, and Carbohydrate Bioproduct Research Center, Seoul 05006, Republic of Korea (W. Lim). Department of Food Science & Biotechnology, Sejong University, Seoul 05006, Republic of Korea, Department of Food Science & Biotechnology, and Carbohydrate Bioproduct Research Center, Seoul 05006, Republic of Korea (T.-G. Lim).

E-mail addresses: wlim@sejong.ac.kr (W. Lim), tglim@sejong.ac.kr (T.-G. Lim).

https://doi.org/10.1016/j.jff.2023.105813
Received 4 July 2023; Received in revised form 1 September 2023; Accepted 21 September 2023
Available online 28 September 2023

compounds (Kumar, Srivastav, & Sharanagat, 2021; Panda & Manickam, 2019). Cavitation, a phenomenon whereby high temperature, pressure, and kinetic energy are generated through ultrasound treatment destroys and penetrates the cell wall and cell membrane to effectively dissolve intracellular compounds, including antioxidants and bioactive substances. Previous studies have reported that UAE could be an environmental and economical technology with promising potential and is expected to be applied to more studies using natural plant-based products (Ranjha et al., 2021).

Pumpkin is rich in β-carotene and vitamins C and E and is known to have beneficial effects on osteoporosis and hypertension (Hussain et al., 2022). Pumpkin tendrils are green vines similar to springs or coils and are agricultural byproducts that are discarded after harvesting pumpkin fruits or leaves for food. However, these agricultural byproducts, which are considered useless and discarded, may contain additional antioxidants and bioactive substances. To date, the functionality of pumpkin tendrils has only been investigated for anti-inflammatory purposes (Jeong et al., 2017). Therefore, in this study, we explored whether pumpkin tendril, an agricultural byproduct, has beneficial effects on skin health.

This study aimed to investigate the anti-melanogenic effects of ultrasound-assisted pumpkin tendril extract on melanoma cells, zebrafish, and a human skin model. These studies on skin-whitening ingredients using pumpkin tendrils are expected to be used to develop eco-friendly materials that can increase economic and environmental value as part of food upcycling.

2. Materials and methods

2.1. Reagents and antibodies

2,2-Diphenyl-1-picrylhydrazyl (DPPH) was purchased from Cayman Chemicals (Ann Arbor, MI, USA). L-DOPA, quercetin, gallic acid, Folin–Ciocalteu phenol reagent, and α-melanocyte stimulating hormone (α-MSH) were obtained from Sigma-Aldrich (St. Louis, MO, USA). Antibodies against TRP-1, MITF, and vinculin were purchased from Santa Cruz Biotechnology (Dallas, TX, USA). Antibodies against TRP-2 and tyrosinase were obtained from Abcam (Cambridge, UK). Anti-phospho-CREB antibody was purchased from Cell Signaling Technology (Danvers, MA, USA). Horseradish peroxidase-conjugated anti-mouse and anti-rabbit secondary antibodies were purchased from Thermo Scientific (Waltham, MA, USA).

2.2. Preparation of pumpkin tendril extract (PTE) by ultrasound-assisted extraction

Fifteen grams of pumpkin tendril (Muan-gun, Jeollanam-do, Republic of Korea) were mixed with 300 mL of 70% ethanol and extracted using an ultrasound processor (Sonics & Materials Inc., Newton, CT, USA) at 34℃ for 1 h. The ultrasound extraction conditions were set to a 30% amplitude, 20 s pulse, 20 Hz frequency, and 750 W maximum power. The extract was filtered through No.41 filter paper (Whatman, Buckinghamshire, UK), evaporated, and freeze-dried (Fig. S1). The yield was calculated as the weight (%, w/w) of the dry extract relative to the dry weight of the pumpkin tendrils. The yield of the PTE was 36.32%, and it was stored at −70℃ until used in subsequent experiments.

2.3. Total phenolic content (TPC) assay

The total phenolic content of the PTE was assessed using the Folin–Ciocalteu reagent whereby. 40 μL of PTE, 20 μL of 1 N Folin-Ciocalteu reagent, and 60 μL of 20% (w/v) Na_2CO_3 were each mixed in a 96-well plate. The mixture was incubated at room temperature for 30 min, and the absorbance was measured at 700 nm. The TPC of the PTE was calculated as milligrams of gallic acid equivalent per gram weight (mg GAE/g) using a gallic acid standard.

2.4. Total flavonoid content (TFC) assay

The total flavonoid content was determined using a modified aluminum chloride method, (Han et al., 2018). whereby 25 μL of PTE, 125 μL of distilled water, and 8 μL of $NaNO_2$ (1 M) were each mixed in a 96-well plate. After reacting for 5 min using an orbital shaker, 15 μL of 10% (w/v) $AlCl_3$ was added to the mixture for 6 min using a shaker, followed by the addition of 50 μL of NaOH (1 M) and 27 μL of distilled water. After the mixture was allowed to react in the dark using a shaker, the absorbance was measured at 510 nm. The TFC of the PTE was calculated as milligrams of quercetin equivalent per gram weight (mg QE/g) using a quercetin standard.

2.5. DPPH assay

To measure the DPPH free radical scavenging activity of PTE, 0.2 mM 2,2-diphenyl-1-picrylhydrazyl (DPPH) dissolved in 99% methanol was prepared. Then, 80 μL of PTE (25–800 μg/mL) was mixed with 80 μL of the DPPH solution in a 96-well plate. After incubating the mixture for 30 min in the dark on a shaker, the absorbance was measured at 517 nm using a microplate reader.

2.6. Mushroom tyrosinase activity assay

To assay the tyrosinase activity of PTE, 80 μL of distilled water, 80 μL of mushroom tyrosinase (27.8 U/mL), and 160 μL of PTE were mixed in a 24-well plate. The mixture was pre-incubated for 10 min using a shaker in the dark and reacted with 40 μL of 3,4-dihydroxy-L-phenylalanine (L-DOPA) (1 mM) as a substrate at room temperature for 30 min in the dark. The concentration of dopachrome as a final product was measured at 475 nm using a microplate reader.

2.7. Cell culture

Murine B16F10 melanoma cells were purchased from the Korean Cell Line Bank (Seoul, Republic of Korea). The cells were cultured in Dulbecco's modified Eagle's medium (DMEM) (HyClone, Logan, UT, USA) supplemented with 10% fetal bovine serum, 100 U/mL penicillin, and 100 μg/mL streptomycin (GIBCO, Waltham, MA, USA) in a humidified incubator at 37 °C and 5% CO_2 atmosphere.

2.8. Cell viability assay

To determine whether PTE affects the viability of B16F10 melanoma cells, an MTS [3-(4,5-dimethylthhylthiazol-2-yl)-5-(3-carboxymethoxyphenyl)-2-(4-sulfophenyl)–2H-tetrazolium] assay was performed. The cells were seeded in a 96-well plate and cultured until they reached 100% confluence. The cells were treated with PTE at concentrations of 12.5–800 μg/mL for 72 h and then reacted with MTS solution for 30 min. The cell viability was determined by measurement of the light absorbance at 490 nm.

2.9. Melanin secretion assay

B16F10 melanoma cells were seeded in a 60 mm dish at a density of 3.0×10^5 cells/dish. After incubation for 16 h, the cells were pretreated with PTE (25–100 μg/mL) for 1 h and stimulated with 100 nM α-melanocyte-stimulating hormone (α-MSH) (Sigma-Aldrich) for 72 h. The supernatant containing melanin was photographed and absorbance was measured at a wavelength of 490 nm.

2.10. Melanin contents assay

B16F10 melanoma cells were seeded in a 60 mm dish at a density of 3.0×10^5 cells/dish. After incubation for 16 h, the cells were pretreated with PTE (25–100 μg/mL) for 1 h and stimulated with 100 nM-MSH for

72 h. The cells were then lysed using trypsin-EDTA (Sigma-Aldrich) and centrifuged, and the supernatant was removed and solubilized in 1 N NaOH at 80 °C for 1 h. The absorbance of the supernatant was measured at 490 nm.

2.11. L-DOPA staining

B16F10 melanoma cells were seeded in a 60 mm dish at a density of 3.0×10^5 cells/dish. After overnight incubation, the cells were pre-treated with PTE (25–100 μg/mL) for 1 h. DMEM supplemented with 100 nM-MSH was then added and further incubated for 72 h. Cells were lysed with cell lysis buffer (Cell Signaling Technology, Danvers, MA, USA) and quantified using the Pierce™ BCA Protein Assay Kit (Thermo Scientific, Waltham, MA, USA). Quantified proteins were separated on 10% sodium dodecyl sulfate–polyacrylamide gels (Bio-Rad Laboratories, Hercules, California, USA). The gel was washed using 0.1 M sodium phosphate monobasic buffer. Then, L-DOPA (10 mM) was added and reacted in a shaking water bath at 37 °C for 2 h.

2.12. Melanin secretion assay in 3D-cultured melanocytes

B16F10 melanoma cells at a 1.0×10^4 cells/well density were seeded into ultra-low attachment 96-well plates (SPL Life Bioscience, Seongnam, Republic of Korea) to form 3D spheroids. After incubation for 16 h, the spherical cells were treated with PTE (25–100 μg/mL) or 200 nM-MSH for 72 h. The 100 μL of supernatant was transferred to a 96-well plate and absorbance was measured at 490 nm.

2.13. Intracellular tyrosinase assay

B16F10 melanoma cells were seeded into a 6-well plate density of 3.0×10^5 cells/well. After overnight incubation, the cells were pre-treated with PTE (25–100 μg/mL) for 1 h and then further treated with 100 nM α-MSH for 72 h. The cells were lysed using a cell lysis buffer (Cell Signaling Technology, Danvers, MA, USA), and the supernatant was collected by centrifugation at 13,000 × g for 10 min. Then, 40 μL of the supernatant and 100 μL of L-DOPA (10 nM) were mixed in a 96-well plate and reacted at 37 °C and 5% CO_2 conditions for 2 h. Intracellular tyrosinase activity was measured by absorbance at 490 nm.

2.14. Western blot analysis

B16F10 melanoma cells were lysed with cell lysis buffer and proteins were quantified using the Pierce™ BCA Protein Assay Kit. Equal amounts of protein were separated on 10% sodium dodecyl sulfate–polyacrylamide gels and transferred to a polyvinylidene difluoride (PVDF) membrane at 25 V for 15 min. The membrane was blocked with 3% bovine serum albumin solution at room temperature for 1 h and incubated with the indicated specific primary antibody at 4 °C for 16 h. The membrane was washed with TBST three times for 10 min each and incubated with a horseradish peroxidase-conjugated secondary antibody for 40 min. After washing the membranes, protein bands were detected using a chemiluminescence reader (LuminoGraph III Lite, ATTO, Tokyo, Japan). Protein expression was calculated using ImageJ software (National Institutes of Health, Bethesda, MD, USA) and compared control set to 1.

2.15. Quantitative real-time PCR

Total RNA was extracted from a 3D pigmented human skin model (Neoderm®-ME) using TRIzol® reagent. The extracted RNA was synthesized into cDNA using the amfiRivert cDNA Synthesis Platinum Master Mix (GenDEPOT, Katy, TX, USA). The primer sequences are shown in Table 1. Quantitative real-time PCR was performed as follows: one cycle of denaturation at 95 °C for 3 min, 40 cycles of denaturation at 95 °C for 15 s, annealing at 58 °C for 15 s, and extension at 72 °C for 30 s.

Table 1
Primer sequence for real-time quantitative PCR.

Genes	Primer sequence (5′-3′)	Product length
MITF (NM_198159.3)	F: GGCATGAACACACATTCACGA R: GGGGCAGACCTTGGTTTCC	184 bp
TRP-1 (NM_000550.3)	F: CTCCAGACAACCTGGGATACAC R: TCAGTGAGGAGAGGCTGGTTA	184 bp
TRP-2 (NM_001322182.2)	F: ATGGGAGGAGGTCTGGTCTG R: GGGCCATCTGACCACTCAAC	121 bp
Tyrosinase (NM_000372.5)	F: GCAAAGCATACCATCAGCTCA R: GCAGTGCATCCATTGACACAT	145 bp
GAPDH (NM_002046.7)	F: GTCTCCTCTGACTTCAACAGCG R: ACCACCCTGTTGCTGTAGCCAA	131 bp

The cycle threshold (Cq) values of each gene were normalized to that of *GAPDH*. The relative expression of the target gene was compared with that of the control set to 1.

2.16. Melanin content assay in reconstituted human tissues

Neoderm®-ME (Tego Science, Seoul, Republic of Korea), a reconstructed three-dimensional human skin model, was used to examine the anti-melanogenesis effect of PTE. Neoderm®-ME is a three-dimensional model containing human primary keratinocytes and melanocytes that mimic human skin. The human skin model was removed from the medium-containing agar, transferred to a 12-well plate, and maintained at 37 °C and 5% CO_2 with PTE (50 and 100 μg/mL) for seven days using the maintenance medium. Arbutin (100 μg/mL) was used as a positive control. To confirm the suppression of melanin production by PTE, microscopic analysis was performed on day 7, and skin darkness was measured using ImageJ software. To analyze the amount of melanin produced in the human skin model, tissue sections were prepared and stained using a Fontana-Masson Staining Kit (Abcam, Cambridge, UK). In brief, the sections were reacted with an ammoniacal silver solution at 60 °C until brown in color, followed by 0.2% gold chloride solution for 30 s and then 5% sodium thiosulfate solution for 1 min. To stain the nuclei, the sections were incubated in nuclear fast red solution for 5 min and quickly dehydrated three times with fresh absolute alcohol. Sections were mounted using a mounting medium (Agilent, Santa Clara, CA, USA) and visualized using a microscope.

2.17. Melanin content assay in zebrafish

Wild-type zebrafish were grown as previously described (Cha, Ko, Kim, & Jeon, 2011). Embryos were collected and raised in the zebrafish embryo medium and then treated with PTE for 8 h after embryonic development. After 72 h of development, the survival rate, hatching rate, and morphological deformities of the PTE-treated group were compared with those of the control group using an EVOS™ XL Core Imaging System (Life Technologies, Bothell, WA, USA). The survival and hatching rates of zebrafish were calculated by counting the number of zebrafish that survived and hatched every day for three days. To evaluate the anti-pigmentation effect of PTE in zebrafish, the zebrafish were treated with PTE for 8 h, and the melanin deposition 72 h after embryogenesis was observed with a microscope. To measure the amount of melanin, the zebrafish were sonicated with 1 × trypsin and centrifuged. The supernatant was removed and the pellet was solubilized in 1 N NaOH at 80 °C for 1 h. The mixture was vortexed vigorously to dissolve the melanin pigment. The absorbance of the supernatant was measured at 475 nm.

2.18. Ultra performance liquid chromatography (UPLC) analysis

PTE was fractionated using an UltiMate™ 3000 HPLC system (Thermo Scientific, Waltham, MA, USA). Solutions of 1% formic acid in water and 0.1% formic acid in acetonitrile were used as the eluents A

and B, respectively. Elution was performed at a flow rate of 0.5 mL/min and different solvent gradients (0–2 min: solvent A 93% and solvent B 7%; 2–11 min: solvent A 93%–83% and solvent B 7%–17%; 11–15 min: solvent A 83%–75% and solvent B 17%–25%; 15–17 min: solvent A 75% and solvent B 25%; 17–20 min: solvent A 75%–93% and solvent B 25%–7%; 20–30 min: solvent A 93% and solvent 7%). Ten microliters of PTE was applied to an Agilent HC-C18 column (4.6 × 250 mm, 5 μm) used for investigation at 259 nm UV wavelength by a UV detector. The column temperature in the instrument was set to 30 °C, and the sample temperature was set to 20 °C. The detection wavelength used for the observation was 259 nm. The rutin peak used in this analysis and each PTE peak were compared with the retention time and expressed as a chromatogram.

2.19. Statistical analysis

All statistical analyses were conducted using SPSS software (version 20.0; SPSS Inc., Chicago, IL, USA). The analyzed data were expressed as mean values ± the standard deviation. Statistical significance was determined using Student's *t*-test for single statistical comparisons, and *P*-values < 0.05 were regarded as significantly different.

3. Results

3.1. Antioxidative activity of PTE

Antioxidants are known to prevent UV-induced excessive melanin production by scavenging reactive oxygen species (Fu et al., 2022). Our

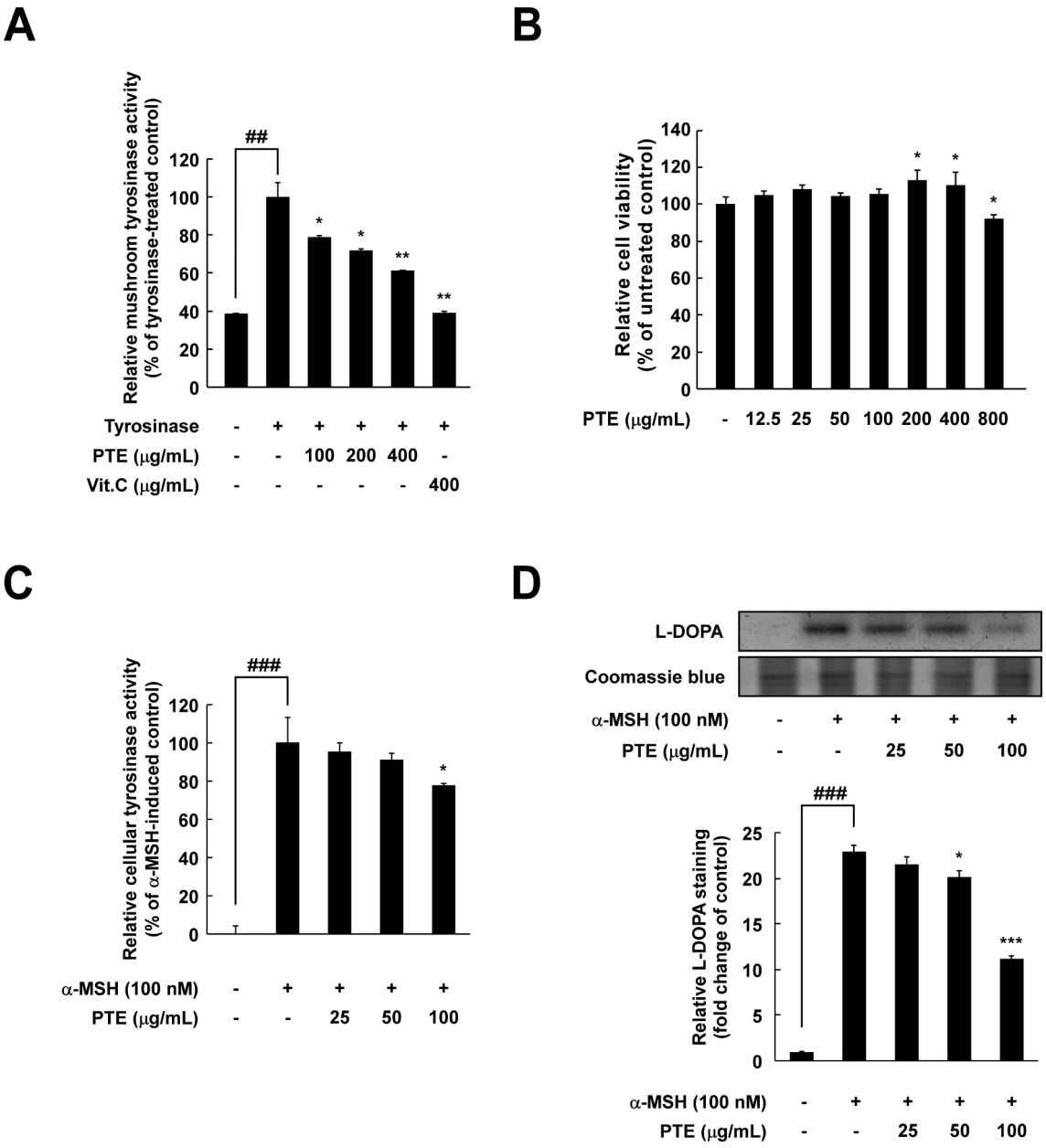

Fig. 1. PTE inhibited tyrosinase activity in murine B16F10 melanoma cells. (A) The effect of PTE on tyrosinase activity was evaluated using a mushroom tyrosinase activity assay. (B) The effect of PTE on B16F10 melanoma cell viability was measured by MTS assay. The cells were treated with the indicated concentration of PTE for 72 h. (C, D) The effect of PTE on intracellular tyrosinase activity in α-MSH-induced B16F10 cells was investigated using a cellular tyrosinase assay and L-DOPA staining. The cells were treated with PTE for 72 h. The data are represented as means ± SD. $^{\#\#}p < 0.01$ and $^{\#\#\#}p < 0.001$ versus the untreated control group; $^{*}p < 0.05$, $^{**}p < 0.01$ and $^{***}p < 0.001$ versus the α-MSH-treated group.

study confirmed the antioxidant effect of PTE by measuring the DPPH free radical scavenging activity as well as the TPC and TFC. PTE was estimated to contain 125.48 ± 4.17 (mg GAE/g) of phenols and 92.73 (mg QE/g) of flavonoids (Table S1). In addition, the DPPH radical-scavenging activity of PTE increased in a dose-dependent manner (Fig. S2). Further exploration of the whitening effect of PTE reflecting an antioxidant effect is hence warranted.

3.2. PTE inhibits tyrosinase activity

Tyrosinase is a key enzyme involved in hyperpigmentation and increased melanin production (Zolghadri et al., 2019). To confirm whether PTE affects melanogenesis, the inhibitory effect of PTE on tyrosinase activity was evaluated using a mushroom tyrosinase inhibition assay. As shown in Fig. 1A, PTE significantly inhibited mushroom tyrosinase activity. The effect of PTE on intracellular tyrosinase activity stimulated by α-MSH in B16F10 cells was also evaluated by L-DOPA staining. In addition, the threshold concentration for PTE cytotoxicity in B16F10 cells was determined by MTS assay. PTE did not exhibit significant changes of viability at concentrations up to 100 μg/mL in B16F10 cells (Fig. 1B). Intracellular tyrosinase activity stimulated by α-MSH was inhibited by PTE treatment in a dose-dependent manner (Fig. 1C and D). Therefore, PTE exerts a suppressive effect on tyrosinase activity without cytotoxicity.

3.3. PTE reduces α-MSH-stimulated melanin production in B16F10 melanoma cells

To investigate the effect of PTE on the inhibition of melanogenesis, the production and secretion of melanin were measured in 2D and 3D culture models of B16F10 cells. As shown in Fig. 2A, PTE inhibited the production of intracellular melanin stimulated by α-MSH. Additionally, extracellular melanin secretion was suppressed by PTE treatment (Fig. 2B). In the 3D culture model using B16F10 cells, the hanging-drop method was used to aggregate the cells. Aggregate formation and growth were confirmed by microscopy. After culture, B16F10 cells were

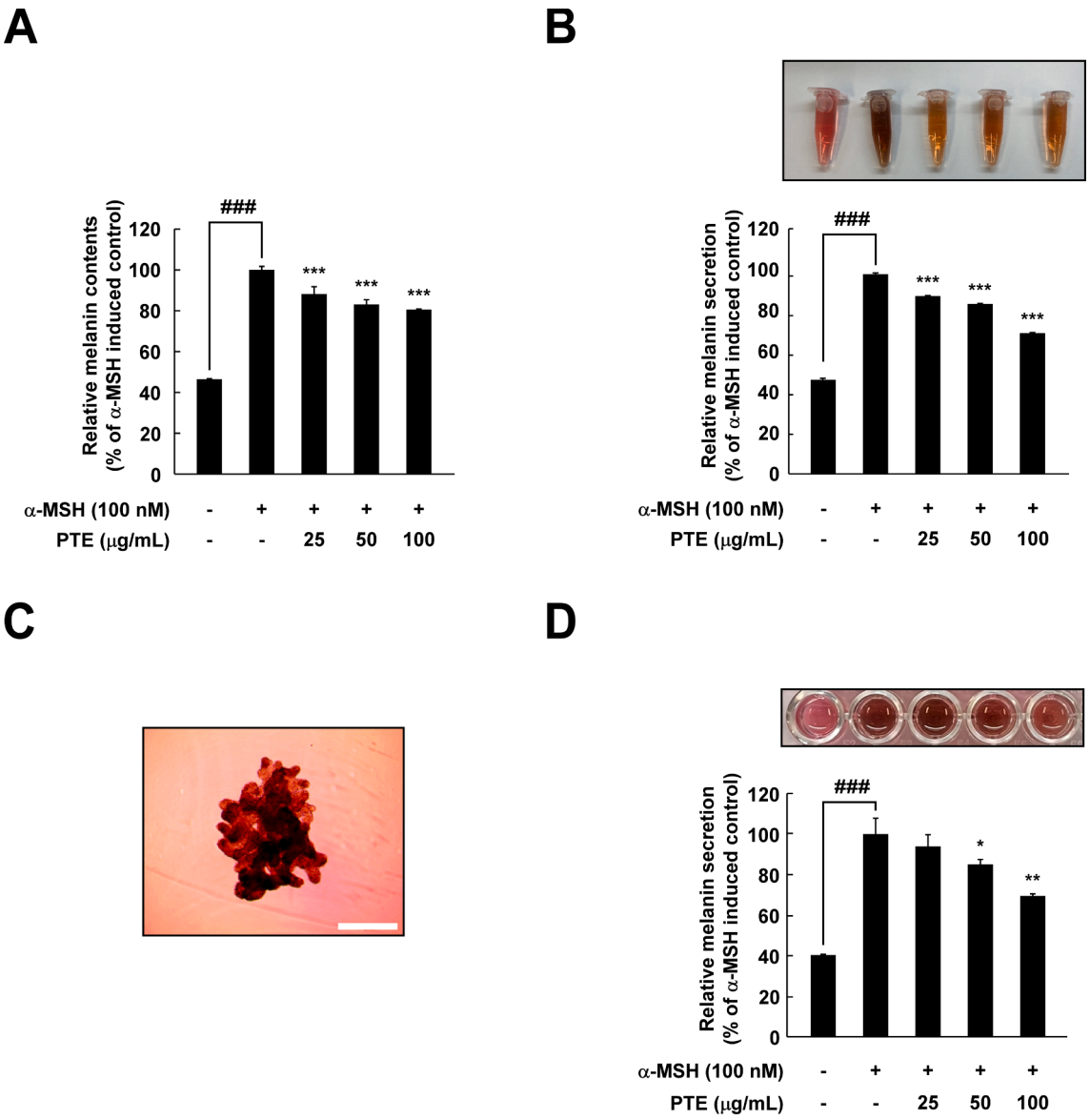

Fig. 2. Effect of PTE on B16F10 melanoma cell melanin accumulation and secretion. (A) Intracellular melanin contents and (B) melanin secretion were evaluated in B16F10 cells after treatment with PTE for 72 h. The data are presented as the absorbance at 490 nm. (C) Morphological assessment of B16F10 spheroids stimulated by α-MSH for 72 h. The scale bar represents 100 μm. (D) Effect of PTE on melanin secretion in 3D-cultured B16F10 cells stimulated by α-MSH. The data are represented as means ± SD. $^{###}p < 0.001$ versus the untreated control group; $^{*}p < 0.05$, $^{**}p < 0.01$ and $^{***}p < 0.001$ versus the α-MSH-treated group.

scattered owing to gravity and moved to the lower side. The cells became aggregated after 12 h and cultured for a further 72 h (Fig. 2C). PTE significantly reduced melanin production and secretion in 3D culture (Fig. 2D). Taken together, these results indicate that melanogenesis and secretion were inhibited by PTE in a dose-dependent manner.

3.4. Down-regulation of tyrosinase, TRP-1, TRP-2, MITF, and CREB protein expression by PTE in B16F10 melanoma cells

Melanin synthesis is regulated by TRP-1, TRP-2, tyrosinase, MITF, and CREB (D'Mello et al., 2016). To determine whether PTE, which has an inhibitory effect on tyrosinase activity, affects the expression of factors involved in melanin synthesis, we assayed for changes in the protein expression of markers and their upstream regulators associated with melanin synthesis by western blot analysis. As shown in Fig. 3A, the protein expression levels of TRP-1, TRP-2, tyrosinase, and MITF were significantly reduced by PTE treatment in a dose-dependent manner. Phosphorylation of CREB, an upstream regulator of MITF, was also decreased by PTE treatment (Fig. 3B). Overall, PTE significantly inhibited TRP-1, TRP-2, tyrosinase, MITF, and p-CREB expression. These results indicated that PTE can suppress melanogenesis by inactivating the CREB/MITF signaling pathway.

3.5. Anti-melanogenesis effect of PTE in a human skin model

Based on the whitening effect of PTE *in vitro*, to confirm the anti-melanogenic effect of PTE in human skin, a three-dimensional human skin model reconstruction whereby human primary keratinocytes and melanocytes were treated with PTE for 7 days. As shown in Fig. 4A, PTE reduced skin darkening in a dose-dependent manner compared to the control group. In particular, the darkening of human skin treated with 100 μg/mL PTE was similar to that of the arbutin-treated group (Fig. 4A). In addition, the mRNA expression levels of melanogenesis-associated biomarkers in human skin tissues were evaluated by RT-PCR. PTE suppressed the expression of *MITF* and *TRP-1* mRNA in a concentration-dependent manner and decreased the mRNA expression of *TRP-2*, and *tyrosinase* at high concentrations (Fig. 4B). These findings indicate that PTE effectively inhibits transcription factors associated with melanogenesis in a human skin model. To observe melanin accumulation in the human skin model, Fontana-Masson staining was performed. As shown in Fig. 4C, PTE decreased melanin pigmentation in a concentration-dependent manner, similar to the arbutin-treated group.

3.6. Effect of PTE on melanin accumulation in zebrafish embryos in vivo

Zebrafish is a well-established model for the evaluation of the skin-whitening effect of cosmeceutical candidates in preclinical dermatology research (Lajis, 2018). The survival and hatching rates of the zebrafish embryos were monitored for 72 h after treatment with PTE. PTE was non-toxic up to 100 μg/mL, and no malformations were observed (Fig. 5A). We further tested whether the reduction in melanin accumulation by PTE was caused by a reduced melanin content, as observed in cultured B16F10 cells. The effect of PTE was observed in PTE-treated zebrafish by microscopy. Melanin accumulation in zebrafish was found to be notably suppressed by PTE treatment in a dose-dependent manner, and PTE decreased the melanin content between $59.64 \pm 0.92\%$ and $70.50 \pm 0.81\%$ compared to the control (Fig. 5B and C). These results further support the *in vitro* findings of the whitening effect of PTE.

3.7. Identification of active compound from PTE using UPLC

UPLC-UV analysis was performed to identify the active compounds responsible for the skin-whitening effects of PTE. Three linear regression equations were generated that correlated the peak areas and concentrations using standard curves for rutin standards. The chromatogram obtained for the standard material using UPLC at a wavelength of 259 nm is shown in Fig. 6. A peak detected in PTE with a retention time similar to that of the rutin standard was determined at a retention time of 23.5 min and a concentration of 239.9 μg/g (Table 2). These findings suggest that PTE contains rutin, which has been suggested to be a functional whitening substance in previous studies and is an anti-melanogenic substance.

4. Discussion

Pumpkin tendril is one of the agricultural byproducts generated during the processing of pumpkin fruits and leaves and is mainly used as food in pumpkin. A number of studies have been conducted to utilize the byproducts of pumpkins, but only anti-inflammatory effects have been reported (Jeong et al., 2017). Recently, as the upcycling trend has spread to various industrial markets in terms of eco-friendliness, research on the development of cosmetic substances using agricultural byproducts such as sugarcane, grape pomace, and walnut shells has attracted considerable attention (Costa et al., 2022; Ferreira & Santos, 2022; Gordobil, Olaizola, Banales, & Labidi, 2020). This study presents evidence for the possibility of high value-added creation of pumpkin tendrils through research on the whitening effects of pumpkin tendrils, which are an agricultural byproduct. In this study, we evaluated the inhibitory effects of extracts derived from pumpkin leaves, seeds, and tendrils, which are primarily generated as by-products during the pumpkin flesh extraction process, on melanogenesis. This assessment was conducted through assays measuring mushroom tyrosinase activity, extracellular melanin secretion activity, and intracellular tyrosinase activity. As a result, pumpkin tendril extract showed the highest inhibitory activity against melanin production and secretion (Fig. S3A–C). Therefore, as a skin-whitening material made from pumpkin-derived by-products, the pumpkin tendril extract was used for the subsequent experiments.

As mentioned earlier, UAE is an extraction technique suitable for the effective separation of bioactive compounds. Numerous research studies are currently in progress to investigate the optimal conditions for efficiently separating functional components through the application of ultrasound-assisted extraction (Fırat, Koca, & Kaymak-Ertekin, 2023; Nurkhasanah, Fardad, Carrera, Setyaningsih, & Palma, 2023; Phuangjit, Klinkesorn, Tan, & Katekhong, 2023). In this study, the utilization of ultrasound-assisted extraction for obtaining pumpkin tendril extract demonstrated notably higher mushroom tyrosinase inhibitory activity in comparison to the traditional heating-based extraction method (Fig. S3D). This outcome strongly suggests the potential utility of ultrasound-assisted extraction for the generation of value-added by-products.

External factors such as ultraviolet rays, smoking, and environmental pollutants increase oxidative stress in the body, resulting in skin aging such as melasma, freckles, age spots, and other hyperpigmentation syndromes (D'Mello et al., 2016; Papaccio, A, Caputo, & Bellei, 2022). As the generation of oxidative stress in melanocytes is mainly induced by ROS, ROS modulators are potential melanogenesis inhibitors. Antioxidants such as vitamins C and E are known to reduce hyperpigmentation caused by ultraviolet rays (Yamakoshi et al., 2003). A number of studies have shown that when the skin is exposed to UV rays, excess hydrogen peroxide is generated, which produces large amounts of α-MSH, which stimulates melanocortin-1 receptor (MC1R) in melanocytes and ultimately increases eumelanin production. In addition, UV radiation enhances ROS production in keratinocytes and melanocytes, DNA damage, and activation of p53, thereby triggering melanogenesis (Kumari, Tien Guan Thng, Kumar Verma, & Gautam, 2018). In this study, PTE exhibited significant DPPH free radical scavenging activity (Fig. S2) and was presumed to inhibit melanin synthesis through ROS scavenging. Moreover, activation of the CREB/MITF pathway by α-MSH was significantly reduced by PTE. Furthermore, the expression of TRP-1, TRP-2, and tyrosinase, which are proteins related to melanin

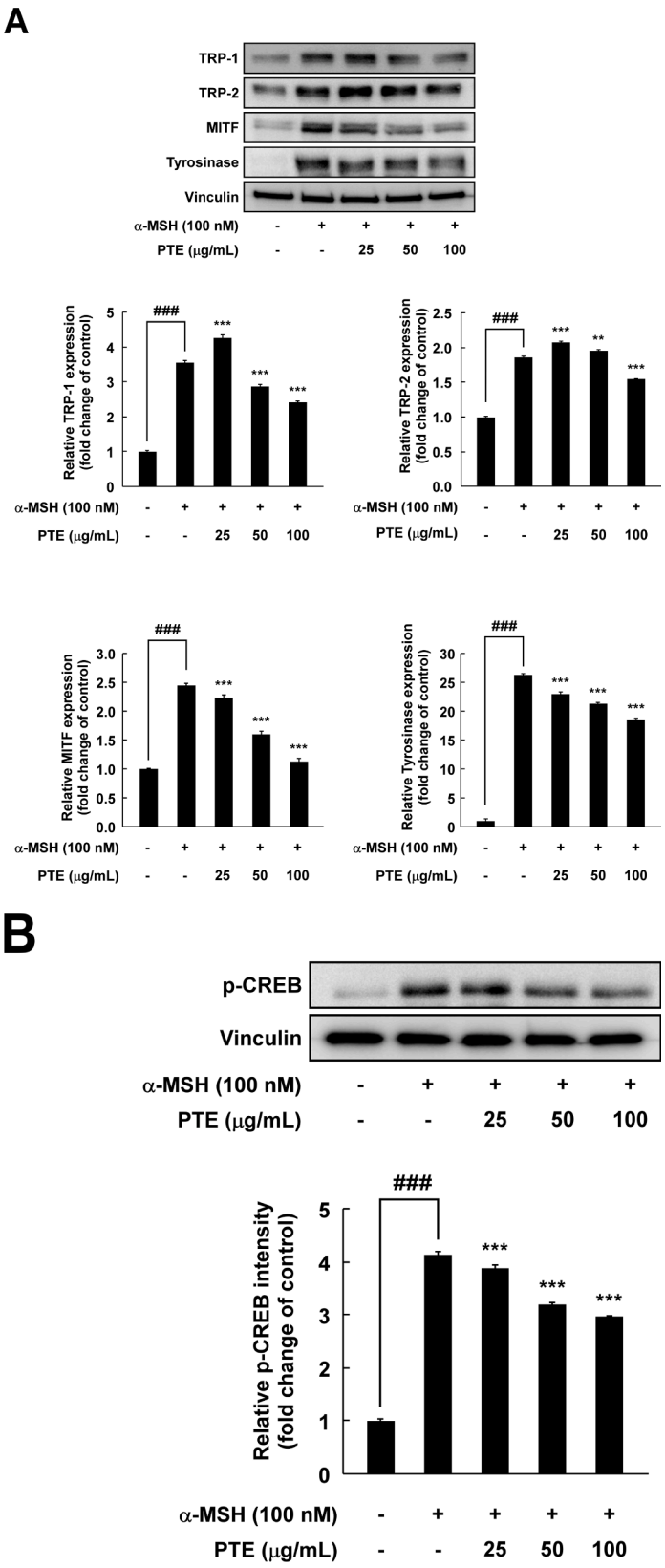

Fig. 3. PTE suppressed melanogenesis stimulated by α-MSH via the MITF/CREB signaling pathway in B16F10 melanoma cells. (A) Cells were treated with PTE for 24 h. Protein expression of TRP-1, TRP-2, MITF, and tyrosinase was determined by western blotting. (B) Cells were treated with PTE for 6 h. Phosphorylation of CREB was measured by western blotting. The relative protein expression was calculated using ImageJ software. The data are represented as means ± SD. $^{###}p < 0.001$ versus the untreated control group; $^{***}p < 0.001$ versus the α-MSH-treated group.

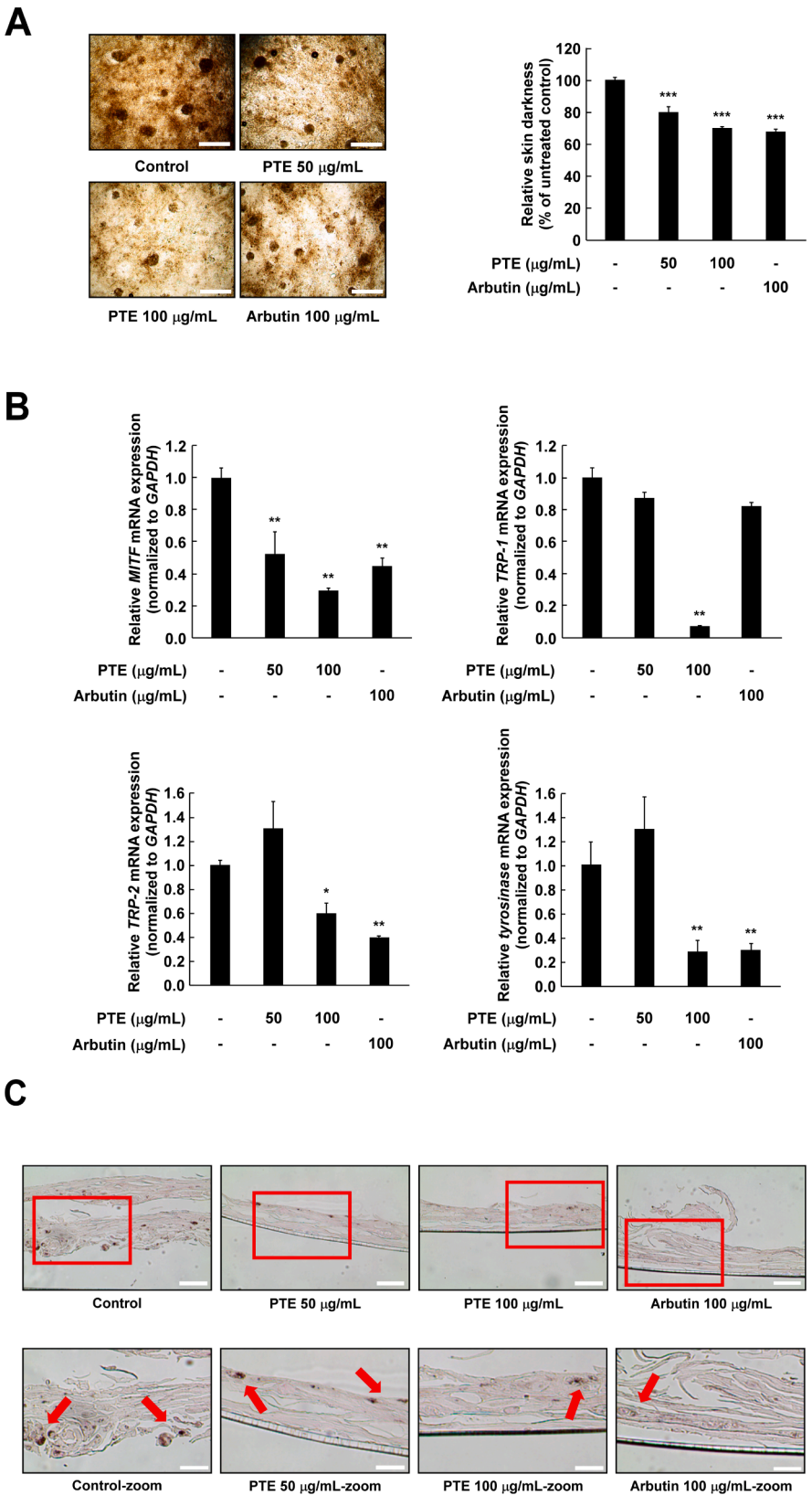

Fig. 4. Anti-melanogenic effect of PTE in a reconstituted 3D human skin model. (A) Three-dimensional human skin was treated with PTE for 7 d. Arbutin was used as a positive control. Skin darkness was observed under a microscope at 100 × magnification and analyzed using ImageJ software. (B) The *MITF*, *TRP-1*, *TRP-2*, and tyrosinase mRNA expression was measured by qRT-PCR. (C) Histological observation of melanin in 3D human skin by Fontana-Masson staining. The scale bar represents 100 μm. The data are represented as means ± SD. $^{*}p < 0.05$ and $^{**}p < 0.01$ versus the untreated control group.

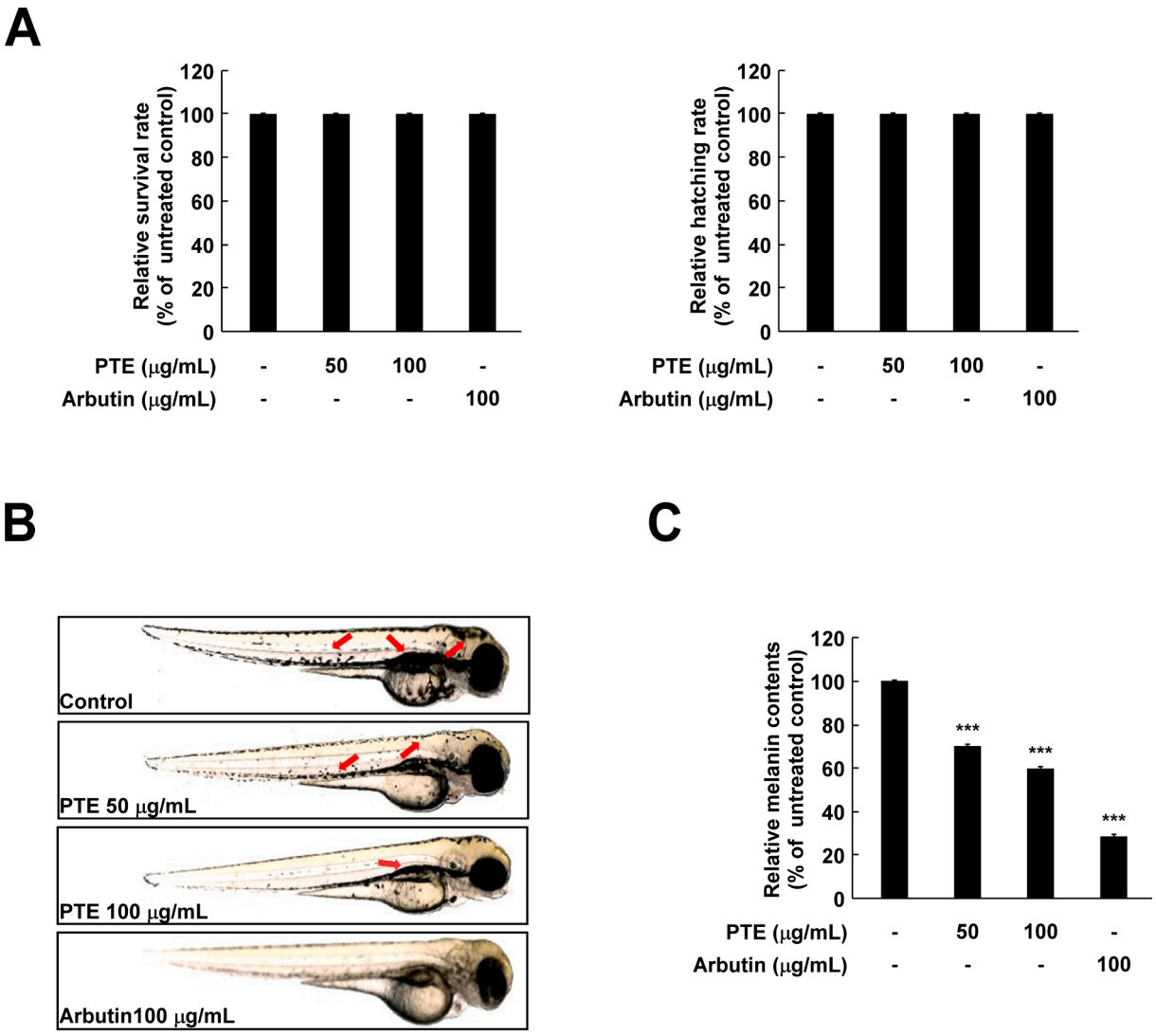

Fig. 5. PTE inhibited melanin synthesis in developing zebrafish embryos. (A) Relative survival and relative hatching rates were investigated after PTE treatment for 72 h. (B) Microscopic observation of melanin accumulation in zebrafish after PTE treatment for 72 h. (C) To measure the melanin content of zebrafish, they were lysed and dissolved in 1 N NaOH to measure the absorbance at 475 nm. The data are represented as means ± SD. $^{***}p < 0.01$ versus the untreated control group.

synthesis, which are increased via the CREB/MITF pathway, were also inhibited by PTE in a concentration-dependent manner (Fig. 3).

Tyrosinase is an enzyme that plays an important role in melanin production, and a measurement of the activity of this enzyme is commonly performed in the early stages of screening for skin-whitening cosmetic candidates (Fu et al., 2022). During melanin production, tyrosinase hydroxylates L-tyrosine to L-DOPA, and oxidizes L-DOPA to L-dopaquinone, resulting in melanin synthesis (Huang, Chou, Wu, & Chang, 2013). In the present study, PTE inhibited mushroom tyrosinase activity in a concentration-dependent manner (Fig. 1A). In addition, PTE notably suppressed the intracellular tyrosinase activity in murine B16F10 melanoma cells without causing cytotoxicity. The secretion of melanin by melanoma cells following exposure to α-MSH was also reduced by PTE. Thus, we explored how PTE regulates melanogenesis. Recently, in the field of dermatology research, various model systems have been used to study skin biology and disease mechanisms. In this study, the anti-melanogenic effect of PTE was evaluated using a 3D B16F10 cell model that addresses the limitations of 2D culture models by culturing cells in a 3D structure similar to skin tissue. This approach better mimics cellular interactions and the microenvironment (Chung, Lim, & Lee, 2019). As shown in Fig. 2C and D, PTE suppressed the melanin production and secretion induced by α-MSH in 3D culture models (Fig. 2C and D). Several studies have reported that α-MSH binding to the melanocortin 1 receptor (MC1R) activates adenylate cyclase and increases the intracellular cAMP concentration, resulting in activation of cAMP-dependent protein kinase (PKA) and increased MITF nuclear transcription as a result of CREB phosphorylation. MITF increases melanin synthesis by increasing the expression of tyrosinase synthesis-related factors and tyrosinase (D'Mello et al., 2016). PTE significantly inhibited the expression of phospho-CREB, MITF, tyrosinase, and other related factors (Fig. 3). Therefore, PTE was speculated to suppress melanogenesis by regulating the CREB/MITF signaling pathway stimulated by α-MSH.

However, the inhibitory effect of PTE on melanogenesis, although validated at the cellular level, requires preclinical evidence for successful clinical application. Therefore, a reconstituted 3D human skin model was used to verify the results at the cellular level in preclinical studies. The 3D pigmented reconstructed skin model, which accurately replicates histological structures similar to human skin, is utilized for evaluating anti-melanogenic effects by studying pigment translocation and melanin distribution within keratinocytes (Yoon et al., 2003). As shown in Fig. 4, PTE reduced melanin synthesis in the human skin model system and the expression of related factors, including *tyrosinase*, *MITF*, *TRP-1*, and *TRP-2*. Within the melanogenesis pathway, tyrosinase

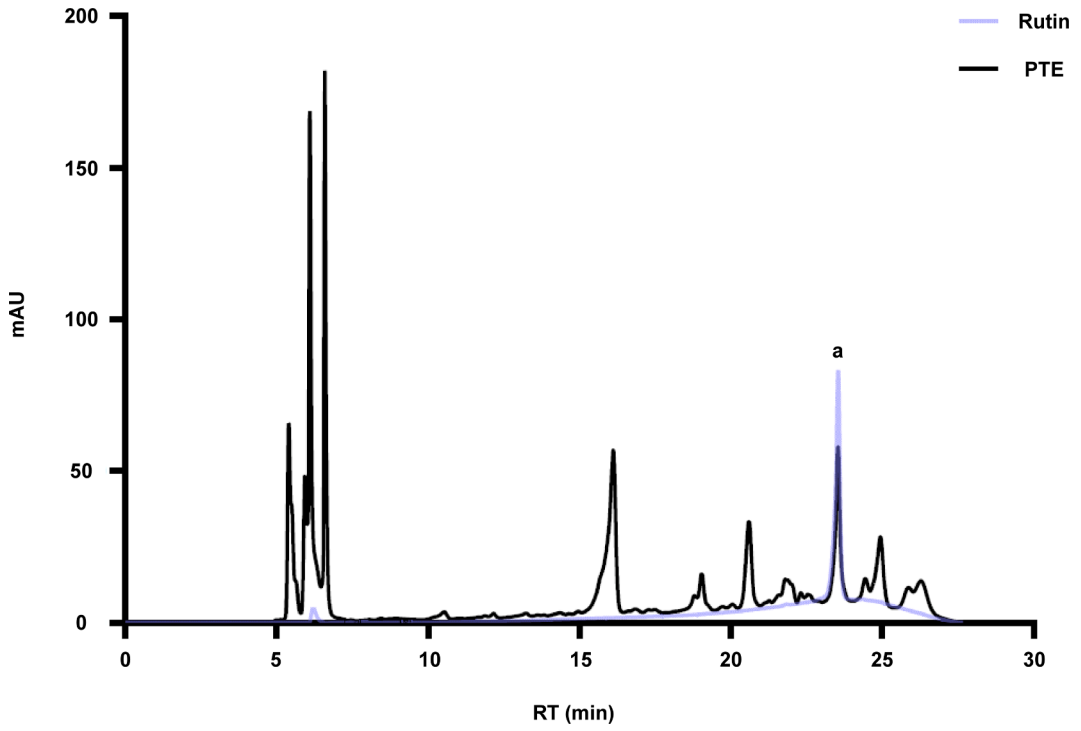

Fig. 6. Identification of rutin as an active component of PTE by UPLC-UV analysis. UPLC chromatograms of PTE were analyzed at 259 nm. The purple peak represents a rutin standard and the black peaks represent PTE. a: rutin.

Table 2
Concentration of rutin from PTE using UPLC.

Compound	Retention time (min)	Concentration (μg/g)
Rutin	23.5	239.9

catalyzes the oxidation of both tyrosine and DOPA. Subsequently, TRP-2 facilitates the conversion of DOPAchrome to DHICA (5,6-dihydroxyindole-2-carboxylic acid), while TRP-1 oxidizes DHICA to ICAQ (indole-2-carboxylic acid-5,6-quinone). Arbutin and PTE suppressed MITF mRNA expression, resulting in the suppression of TRP-1 mRNA expression. We suggest that in a reconstitute human skin model, arbutin and PTE inhibit melanogenesis by inhibiting tyrosine and DOPA oxidation and ICAQ production through mRNA inhibition of tyrosinase and TRP-1. On the other hand, the TRP-2 mRNA expression levels differed between PTE and arbutin. To understand the difference in TRP-2 mRNA expression, further studies on transcription factors other than MITF are necessary (Chang, 2012).

The zebrafish model is well-established for comprehensive skin-related research, including melanin synthesis experiments. Zebrafish possess transparent larvae, enabling real-time observation of internal changes. Moreover, this model offers an improved mimicry of tissue morphology and function, which enhances the reproducibility of biological phenomena (Lajis, 2018). Interestingly, PTE suppressed melanin accumulation in zebrafish in a dose-dependent manner, and the degree of inhibition of melanogenesis in this model system was similar to that of the well-known whitening cosmetic material arbutin.

Although there have been few studies to date on the component analysis of pumpkin tendrils, rutin is a major polyphenol compound that exerts a skin-whitening effect (Si et al., 2012). In this study, UPLC was performed to identify the functional ingredients of pumpkin tendrils that have skin-whitening effects. As shown in Table 2, rutin was detected and identified as one of the ingredients present in PTE, which can be scientific evidence for identifying the active compound responsible for the skin whitening effect of PTE. In a previous study, bamboo stems, including rutin, showed anti-melanogenic activity through down-regulating the CREB/MITF signaling pathway in melanoma cells (Choi, Jo, Yang, Ki, & Shin, 2018). Also, the rutin derived from *Dendropanax morbiferus* was suggested as an active component for anti-melanogenesis through suppressing the CREB/MITF signaling pathway (Park et al., 2020). Taken together, rutin has the potential to be an anti-melanogenic natural component through downregulation of the CREB/MITF signaling pathway. These results suggest that the determination of the rutin content of pumpkin tendrils provides evidence for the standardization of potential raw materials that can have a whitening effect. Further studies are needed to identify the synergistic effects of still-to-be-identified compounds and rutin.

5. Conclusions

In summary, we evaluated the effects of PTE on melanogenesis on mushroom tyrosinase, murine B16F10 cells, reconstituted 3D human skin, and zebrafish models. PTE inhibited the expression of melanogenesis-related factors and tyrosinase activity. Therefore, PTE has a skin-whitening effect and has ample potential for use as a cosmeceutical.

6. Ethics Statement

The research did not include any human subjects and animal experiments hence ethical approval is not required.

CRediT authorship contribution statement

Sujung Hong: Writing – original draft, Formal analysis, Investigation. **Sojeong Lee:** Resources. **Woo-Jin Sim:** Investigation. **Wook Chul Kim:** Formal analysis, Investigation. **Seon-Young Kim:** Funding acquisition. **Mi Hee Park:** Funding acquisition. **Wonchul Lim:** Writing – review & editing, Supervision. **Tae-Gyu Lim:** Project administration, Funding acquisition, Supervision.

Declaration of Competing Interest

The authors declare that they have no known competing financial interests or personal relationships that could have appeared to influence the work reported in this paper.

Data availability

No data was used for the research described in the article.

Acknowledgments

This research was funded by the Ministry of Science and ICT and by the National Research Foundation of Korea (NRF) grant funded by the Korea government (MSIT), grant number 2020R1C1C1004670, by the Bio & Medical Technology Development Program of the National Research Foundation (NRF) funded by the Ministry of Science & ICT (NRF-2022M3A9I5082349). And this research was supported by Basic Science Research Program through the National Research Foundation of Korea (NRF) funded by the Ministry of Education (2022R1A6A1A03055869).

Appendix A. Supplementary material

Supplementary data to this article can be found online at https://doi.org/10.1016/j.jff.2023.105813.

References

Cha, S. H., Ko, S. C., Kim, D., & Jeon, Y. J. (2011). Screening of marine algae for potential tyrosinase inhibitor: Those inhibitors reduced tyrosinase activity and melanin synthesis in zebrafish. *Journal of Dermatology, 38*(4), 343–352. https://doi.org/10.1111/j.1346-8138.2010.00983.x

Chang, T.-S. (2012). Natural melanogenesis inhibitors acting through the down-regulation of tyrosinase activity. *Materials, 5*(9), 1661–1685. https://doi.org/10.3390/ma5091661

Choi, M. H., Jo, H. G., Yang, J. H., Ki, S. H., & Shin, H. J. (2018). Antioxidative and Anti-Melanogenic Activities of Bamboo Stems (Phyllostachys nigra variety henosis) via PKA/CREB-Mediated MITF Downregulation in B16F10 Melanoma Cells. *International Journal of Molecular Sciences, 19*(2), 409. https://doi.org/10.3390/ijms19020409

Chung, S., Lim, G. J., & Lee, J. Y. (2019). Quantitative analysis of melanin content in a three-dimensional melanoma cell culture. *Scientific Reports, 9*(1), 780. https://doi.org/10.1038/s41598-018-37055-y

Costa, J. R., Capeto, A. P., Pereira, C. F., Pedrosa, S. S., Mota, I. F., Burgal, J. D. S., … Madureira, A. R. (2022). Valorization of Sugarcane By-Products through Synthesis of Biogenic Amorphous Silica Microspheres for Sustainable Cosmetics. *Nanomaterials, 12*(23), 4201. https://doi.org/10.3390/nano12234201

D'Mello, S. A., Finlay, G. J., Baguley, B. C., & Askarian-Amiri, M. E. (2016). Signaling Pathways in Melanogenesis. *International Journal of Molecular. Science, 17*(7). https://doi.org/10.3390/ijms17071144

Ferreira, S. M., & Santos, L. (2022). A Potential Valorization Strategy of Wine Industry by-Products and Their Application in Cosmetics-Case Study: Grape Pomace and Grapeseed. *Molecules, 27*(3), 969.

Fırat, E., Koca, N., & Kaymak-Ertekin, F. (2023). Extraction of pectin from watermelon and pomegranate peels with different methods and its application in ice cream as an emulsifier. *Journal of Food Science*. https://doi.org/10.1111/1750-3841.16752

Fu, W. C., Wu, Z. F., Zheng, R., Yin, N., Han, F. J., Zhao, Z. Z., … Niu, L. (2022). Inhibition mechanism of melanin formation based on antioxidant scavenging of reactive oxygen species. *The Analyst, 147*(12), 2703–2711. https://doi.org/10.1039/D2AN00588C

Gordobil, O., Olaizola, P., Banales, J. M., & Labidi, J. (2020). Lignins from Agroindustrial by-Products as Natural Ingredients for Cosmetics: Chemical Structure and In Vitro Sunscreen and Cytotoxic Activities. *Molecules, 25*(5), 1131. https://doi.org/10.3390/molecules25051131

Han, Z., Zhang, J., Cai, S., Chen, X., Quan, X., & Zhang, G. (2018). Association mapping for total polyphenol content, total flavonoid content and antioxidant activity in barley. *BMC Genomics, 19*(1), 81. https://doi.org/10.1186/s12864-018-4483-6

Huang, H. C., Chou, Y. C., Wu, C. Y., & Chang, T. M. (2013). [8]-Gingerol inhibits melanogenesis in murine melanoma cells through down-regulation of the MAPK and PKA signal pathways. *Biochemical and Biophysical Research Communications, 438*(2), 375–381. https://doi.org/10.1016/j.bbrc.2013.07.079

Hussain, A., Kausar, T., Sehar, S., Sarwar, A., Ashraf, A. H., Jamil, M. A., … Majeed, M. A. (2022). A Comprehensive review of functional ingredients, especially bioactive compounds present in pumpkin peel, flesh and seeds, and their health benefits. *Food Chemistry Advances, 1*, Article 100067. https://doi.org/10.1016/j.focha.2022.100067

Jeong, H.-N., Choi, J.-H., Lee, H.-N., Lee, S.-H., Cho, S.-C., Park, J.-H., & Kim, Y.-M. (2017). Inflammation inhibitory effect of water extract from pumpkin's tendril. *Korean Journal of Food Preservation, 24*(8), 1122–1128. https://doi.org/10.11002/kjfp.2017.24.8.1122

Kumar, K., Srivastav, S., & Sharanagat, V. S. (2021). Ultrasound assisted extraction (UAE) of bioactive compounds from fruit and vegetable processing by-products: A review. *Ultrasonics Sonochemistry, 70*, Article 105325. https://doi.org/10.1016/j.ultsonch.2020.105325

Kumari, S., Thng, T. G., Kumar, S., Verma, N., & Gautam, H. K. (2018). Melanogenesis Inhibitors. *Acta Dermato-Venereologica, 98*(10), 924–931. https://doi.org/10.2340/00015555-3002

Lajis, A. F. B. (2018). A Zebrafish Embryo as an Animal Model for the Treatment of Hyperpigmentation in Cosmetic Dermatology Medicine. *Medicina-Lithuania, 54*(3), 35. https://doi.org/10.3390/medicina54030035

Nurkhasanah, A., Fardad, T., Carrera, C., Setyaningsih, W., & Palma, M. (2023). Ultrasound-Assisted Anthocyanins Extraction from Pigmented Corn: Optimization Using Response Surface Methodology. *Methods and Protocols, 6*(4), 69. https://doi.org/10.3390/mps6040069

Panda, D., & Manickam, S. (2019). Cavitation Technology-The Future of Greener Extraction Method: A Review on the Extraction of Natural Products and Process Intensification Mechanism and Perspectives. *Applied Sciences-Basel, 9*(4), 766. https://doi.org/10.3390/app9040766

Papaccio, F., A, D. A., Caputo, S., & Bellei, B. (2022). Focus on the Contribution of Oxidative Stress in Skin Aging. Antioxidants, 11(6), 1121. https://doi.org/10.3390/antiox11061121.

Park, J. U., Yang, S. Y., Guo, R. H., Li, H. X., Kim, Y. H., & Kim, Y. R. (2020). Anti-Melanogenic Effect of Dendropanax morbiferus and Its Active Components via Protein Kinase A/Cyclic Adenosine Monophosphate-Responsive Binding Protein- and p38 Mitogen-Activated Protein Kinase-Mediated Microphthalmia-Associated Transcription Factor Downregulation. *Frontiers in Pharmacology, 11*, 507. https://doi.org/10.3389/fphar.2020.00507

Phuangjit, U., Klinkesorn, U., Tan, C. P., & Katekhong, W. (2023). Enhancing silkworm protein yield, extraction efficiency, structure, functionality, and antioxidant activity using ultrasound-, microwave-, and freeze-thaw-assisted methods. *Journal of the Science of Food and Agriculture*. https://doi.org/10.1002/jsfa.12929

Ranjha, M. M. A. N., Irfan, S., Lorenzo, J. M., Shafique, B., Kanwal, R., Pateiro, M., … Aadil, R. M. (2021). Sonication, a Potential Technique for Extraction of Phytoconstituents: A Systematic Review. *Processes, 9*(8), 1406. https://doi.org/10.3390/pr9081406

Si, Y. X., Yin, S. J., Oh, S., Wang, Z. J., Ye, S., Yan, L., … Qian, G. Y. (2012). An Integrated Study of Tyrosinase Inhibition by Rutin: Progress using a Computational Simulation. *Journal of Biomolecular Structure & Dynamics, 29*(5), 999–1012. https://doi.org/10.1080/073911012010525028

Solano, F. (2020). Photoprotection and Skin Pigmentation: Melanin-Related Molecules and Some Other New Agents Obtained from Natural Sources. *Molecules, 25*(7), 1537. https://doi.org/10.3390/molecules25071537

Yamaguchi, Y., Brenner, M., & Hearing, V. J. (2007). The regulation of skin pigmentation. *Journal of Biological Chemistry, 282*(38), 27557–27561. https://doi.org/10.1074/jbc.R700026200

Yamakoshi, J., Otsuka, F., Sano, A., Tokutake, S., Saito, M., Kikuchi, M., & Kubota, Y. (2003). Lightening effect on ultraviolet-induced pigmentation of guinea pig skin by oral administration of a proanthocyanidin-rich extract from grape seeds. *Pigment Cell Research, 16*(6), 629–638. https://doi.org/10.1046/j.1600-0749.2003.00093.x

Yoon, T. J., Lei, T. C., Yamaguchi, Y., Batzer, J., Wolber, R., & Hearing, V. J. (2003). Reconstituted 3-dimensional human skin of various ethnic origins as an in vitro model for studies of pigmentation. *Analytical Biochemistry, 318*(2), 260–269. https://doi.org/10.1016/s0003-2697(03)00172-6

Zolghadri, S., Bahrami, A., Khan, M. T. H., Munoz-Munoz, J., Garcia-Molina, F., Garcia-Canovas, F., & Saboury, A. A. (2019). A comprehensive review on tyrosinase inhibitors. *Journal of Enzyme Inhibition and Medicinal Chemistry, 34*(1), 279–309. https://doi.org/10.1080/14756366.2018.1545767